

# Extraction of Conversion Matrices for P-HEMTs based on Vectorial Large-Signal Measurements

A. Cidronali<sup>1</sup>, K.C. Gupta<sup>2</sup>, J. Jargon<sup>3</sup>, K. A. Remley<sup>3</sup>, D. DeGroot<sup>3</sup>, G. Manes<sup>1</sup>

<sup>1</sup>Dept. Electronics and Telecommunications University of Florence, Florence 50139 Italy

<sup>2</sup>University of Colorado at Boulder, Dept. of Electrical and Computer Engineering, USA

<sup>3</sup>National Institute of Standards and Technology, Boulder, CO 80305 USA

**Abstract** — We introduce a new technique which allows us to measure the admittance conversion matrix of a two port device, using a large-signal vector network analyzer. This method is applied to extract the conversion matrix of a 0.25  $\mu\text{m}$  PHEMT, driven by a 4.8 GHz signal, at different power levels, using an intermediate frequency of 600 MHz. A discussion of the up- and down-conversion is provided.

## I. INTRODUCTION

A nonlinear vector network analyzer (NVNA) was recently introduced that can accurately measure the amplitude and phase of a limited number of spectral components of both the complex incident and scattered voltage wave variables. These NVNAs have been used to characterize nonlinear microwave devices and circuits [1]. In the field of modeling, researchers have applied NVNA measurements to the definitions of nonlinear scattering functions [2] and nonlinear large-signal scattering parameters [3], and for directly extracting device state functions [4], to name just a few. The purpose of this paper is to apply large-signal vectorial measurements to the design of a frequency converter. Specifically, we extend a conventional linear design method to a nonlinear circuit in the hopes of achieving an optimum design, and in turn a more efficient system. Our approach will allow us to reduce the requirement of complex nonlinear device models and large-signal analysis by determining the conversion matrix [5]. The results of [5] effectively describe how to apply such a matrix to mixer design. The focus of the present paper is the experimental determination of such a matrix. The characterization method is described and applied to a P-HEMT under large signal pumping, with a number of experimental results describing the potential of this approach for mixer design.

## II. MEASUREMENT SET-UP

The NVNA consists of a 4-channel data acquisition system and provides magnitude and phase values of the incident and scattered complex wave variables at both

ports of the device on a user-defined grid. In particular, it consists of two RF sources, a DC bias supply, four directional couplers, an RF to IF down converter, and a data acquisition system [6]. The two RF sources can be combined to supply the desired excitations at port 1 or port 2. Input and output tuners can be added to control the phase of the multi-tone excitation. An appropriate amplitude and phase calibration procedure allows for the correction of the “raw” quantities. The set-up is shown in Fig.1, where a large pump signal is applied to the DUT's port 1 while a second signal, namely a low-level signal is switched from port 1 and port 2. This operation doesn't substantially change the port impedance.

The NVNA is able to measure both the harmonics of the large signal and the mixing products, provided the calibration grid contains the frequencies of interest.

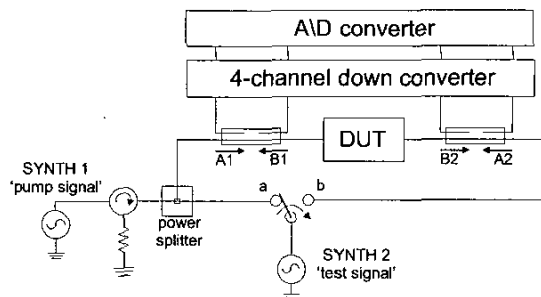


Fig.1 Set-up adopted for the conversion matrix characterization based on the NVNA. (The bias part of the set is not shown.)

## III. EXTRACTION OF THE CONVERSION MATRIX

Let us consider the DUT pumped by a large signal  $S1$  at port 1 whose fundamental frequency is  $F1$  and amplitude  $A1$ . The DUT behavior under this excitation may exhibit harmonic generation. Without further consideration, this set-up is the one considered below.

In the general case of a DUT which contains nonlinear components, a large-signal nonlinear analysis is required to calculate the waveforms at the terminals of the nonlinearities. Consider now the injection of a small signal  $S2$  at a frequency  $F0$  offset from  $F1$ ; the circuit can be treated as linear with parametric elements periodically

\* Work partially supported by an agency of the U.S. Government. Not subject to U.S. Copyright.

varying with time. The resulting intermodulation products (IMPs) contain the frequencies  $nF_1 \pm F_0$ ,  $n = 0, 1 \dots N$ , as shown in Fig.2.

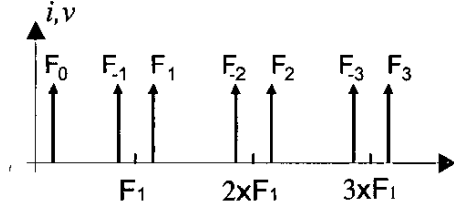


Fig. 2. Spectrum notation of the small-signal IM frequencies.

The well-known large-signal small-signal theory [5] allows us to consider the relationship between voltages and currents of such IMPs, which can be derived from the following conversion matrix:

$$\begin{pmatrix} i_{1,-N}^* \\ \vdots \\ i_{1,0} \\ \vdots \\ i_{1,N} \\ \hline i_{2,-N}^* \\ \vdots \\ i_{2,0} \\ \vdots \\ i_{2,N} \end{pmatrix} = \begin{pmatrix} y_{1,1,-N,-N} & \dots & y_{1,1,-N,N} & \vdots \\ \vdots & \ddots & \vdots & \dots y_{1,2,i,j} \dots \\ y_{1,1,N,-N} & \dots & y_{1,1,N,N} & \vdots \\ \hline y_{2,1,-N,-N} & \dots & y_{2,1,-N,N} & \vdots \\ \vdots & \ddots & \vdots & \dots y_{2,2,i,j} \dots \\ y_{2,1,N,-N} & \dots & y_{2,1,N,N} & \vdots \end{pmatrix} \times \begin{pmatrix} v_{1,-N}^* \\ \vdots \\ v_{1,0} \\ \vdots \\ v_{1,N} \\ \hline v_{2,-N}^* \\ \vdots \\ v_{2,0} \\ \vdots \\ v_{2,N} \end{pmatrix} \quad (1)$$

where  $y_{ijmn} = i_{i,m} / v_{j,n}$  with all the voltage components differing from  $v_{j,n}$ , equal to zero.

Because of the inherent linear nature of the problem, eq. (1) relates the IMPs, in terms of voltages and currents, regardless of their amplitude, provided that they do not excite the nonlinearities of the DUT. This means that (1) allows for the determination of the frequency conversion properties, in the case of an input signal, at any of the frequencies  $nF_1 \pm F_0$ ,  $n = 0, 1 \dots N$ .

The dominant problem of mixer analysis is to determine the coefficients of matrix (1), which is conventionally done by means of nonlinear analysis. For the purpose of an accurate nonlinear model, we must also be able to handle multitone excitations, including the capability of considering memory, thermal, and frequency-dispersive-effects. The availability of equipment such as the NVNA allows us to introduce a new technique for determining the conversion matrix with *experimental* data. The remainder of this paper deals with the description of the extraction technique and experimental results.

From (1) we see that there are  $4(2N+1)^2$  unknowns, represented by  $y_{ijmn}$ , where  $i, j = 1, 2$  and  $m, n = -N, \dots, 0, \dots$ .

Here,  $N$  is the maximum number of harmonics considered in the large-signal analysis. The system of equations is obviously not suitable for determining the coefficients  $y_{ijmn}$ , when there are  $(4N+2)$  equations.

In order to evaluate the coefficients in the conversion matrix we collect  $(4N+2)$  measurements of the IMPs in the same state; i.e. at the same bias point and large-signal level and frequency, but with a small test signal injected at the IMPs, first at port 1 then at port 2. This is easily obtained using the switch depicted in Fig.1. In such a way, there are  $(4N+2)$  sets of currents and voltages related by the conversion matrix. After manipulating these equations, the linear system in (1) is reformulated in terms of the coefficients of the conversion matrix, while the matrix of the linear system is filled with the measured voltages in their proper positions. The system now has dimensions of  $4(2N+1)^2 \times 4(2N+1)^2$  with  $4(2N+1)^2$  unknowns, and can be easily solved by conventional matrix inversion.

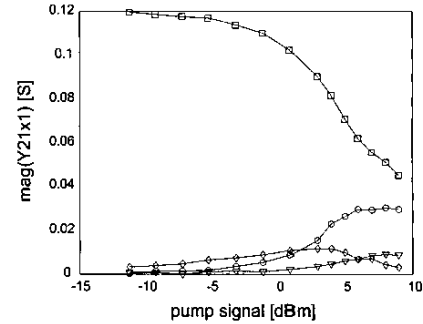


Fig. 3. Magnitude of the coefficients:  $y_{2111}$  (squares),  $y_{2121}$  (diamonds),  $y_{2131}$  (circles) and  $y_{2141}$  (triangles) at  $V_d=3$  V,  $V_g=-0.45$  V.

#### IV. EXPERIMENTAL RESULTS

The technique described above has been applied to extracting the conversion matrix of a 0.25  $\mu\text{m}$  P-HEMT, for a pump signal at 4.8GHz. The experiments have been carried out at power levels ranging from  $-12$  dBm to  $+9$  dBm and for bias points:  $V_d = 3$  V,  $V_g = -0.45, -0.85, -1.2$  V. The NVNA was calibrated with a 600 MHz grid up to 19.8 GHz, with 32 harmonics included. In order to collect an adequate set of small signal components, a test signal of  $-30$  dBm was repetitively applied to port 1 and then port 2 at 600 MHz, 4.2 GHz, 5.4 GHz, 9 GHz, 10.2 GHz, 13.8 GHz, 15 GHz, 18.6 GHz, and 19.8 GHz, (i.e.  $F_1 = 4.8$  GHz and  $F_0 = 600$  MHz and  $N = 4$ ). This power level was selected by trading off between the constraints due to the linearity of the DUT and the dynamic range of the NVNA. The preceding frequency list corresponds to the IMPs when 4 harmonics of the large signal were considered and  $F_0 = 600$  MHz. Measurements of the current and voltages at those frequencies were collected, providing the required

set of data. The operation was repeated similarly for all of the power levels and bias voltages.

In the case of  $N = 4$ , a system of equations is generated with dimension  $324 \times 324$ , where 324 is the size of the array which contains the  $y_{ijm}$  coefficients. Some of these coefficients are worth discussing in detail. For example,  $y_{211}$ , shown in Fig. 3, which is strongly related to the device transconductance  $g_m$  is the ratio between the spectral component for the current at port 2 and the voltage at port 1, both at 5.4GHz. At low levels of the pump signal, its value is similar to that measured by a conventional linear network analyzer. As the pump signal increases, this value decreases as the value of  $y_{21x1}$  (with  $x = 2, 3, 4$ ) increases. This behavior is depicted in Fig. 3, where the magnitudes of the coefficients are plotted as a function of the input power at the fundamental of the large signal, for a bias point corresponding to  $I_{dss}/2$ .

The  $y_{21x1}$  parameters, relate the currents at 10.2 GHz, 15 GHz and 19.8 GHz respectively, with the fundamental voltage at port 1. These components are relatively small since the input power does not create an increase in the higher-order IMPs with a corresponding reduction in the  $y_{211}$  magnitude. Furthermore, above a power level of 2 dBm the third harmonic increases more than the second and fourth. This is due to the particular bias point that determines a symmetric clamping of the output current waveform. All of these behaviors are expected by the device physics.

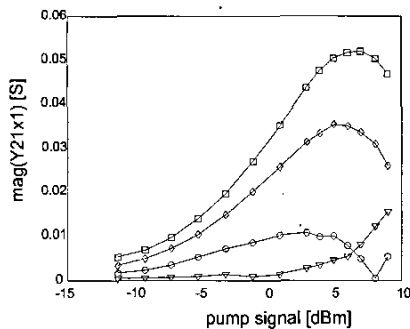


Fig. 4. Magnitude of the coefficients:  $y_{2111}$  (squares),  $y_{2121}$  (diamonds),  $y_{2131}$  (circles) and  $y_{2141}$  (triangles) at  $V_d = 3$  V,  $V_g = -1.2$  V.

Fig. 4 shows the,  $y_{21x1}$  coefficients, at the pinch-off bias point. In this case, the transconductance values at the various IMPs are small for low pump levels, while they increase at high levels. This effect depends on the harmonic generation due to the switching operation mode and is exploited in frequency conversion circuits. Contrary to the previous case,  $y_{2121}$  corresponding to the second harmonic, increases more than the higher-order transconductances, as expected for this particular bias point.

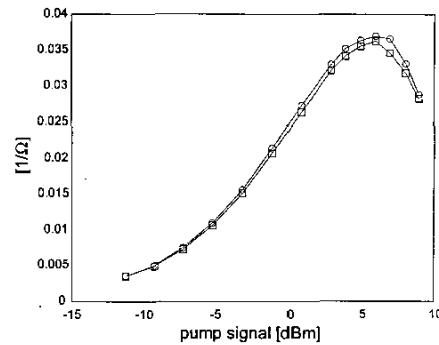


Fig. 5. Magnitude of the coefficients:  $y_{2110}$ , (squares),  $y_{2101}$  (circles) at  $V_d = 3$  V,  $V_g = -1.2$  V.

Next, we inspect the down and up conversions. The mixer analysis using the conversion matrix leads to the expression of the maximum conversion gain (MCG). It relates the power at the input frequency and the power at the output frequency using a basic assumption that the ports are terminated with shorts at the unwanted mixing frequencies [5]. Moreover, in the particular case where  $y_{12xy}$  is negligible, MCG for the up-conversion becomes:

$$MCG = \frac{|y_{2110}|^2}{4 \operatorname{Re}\{y_{1100}\} \operatorname{Re}\{y_{2211}\}} \quad (2)$$

where  $y_{2110}$  is the transconductance, evaluated from the ratio of the output current at 5.4 GHz and the voltage at port 1 at 600 MHz. The parameters  $y_{1100}$  and  $y_{2211}$  represent the input and output admittances at 600 MHz and 5.4 GHz, respectively. The load and input impedances that ensure the MCG, in the unilateral approximation, are the conjugates of  $y_{2211}$  and  $y_{1100}$ , respectively. An analogous result is obtained for the down-conversion case if  $y_{2110}$ ,  $y_{1100}$  and  $y_{2211}$  are replaced by  $y_{2101}$ ,  $y_{1111}$  and  $y_{2200}$  respectively.

We report the magnitude values of  $y_{2110}$  and  $y_{2101}$  at different bias points for pump signal ranging from -12 dBm to +9 dBm. In particular, Fig. 5 shows the conversion parameters between 600 MHz and 5.4 GHz using a pump signal at 4.8 GHz, at a bias point close to pinch-off. At low levels of input power, the two conversion coefficients for the up- and the down-conversions, increase in a similar way, where they reach a maximum near pump levels of 5 dBm. In Fig. 6, similar behavior is observed for a bias point around which the device is approximately linear. For higher input powers we observe an increase of the coefficients associated with the second and third order (not shown here). The maximums, which are lower than the previous case, are reached for approximately the same pump signal power.

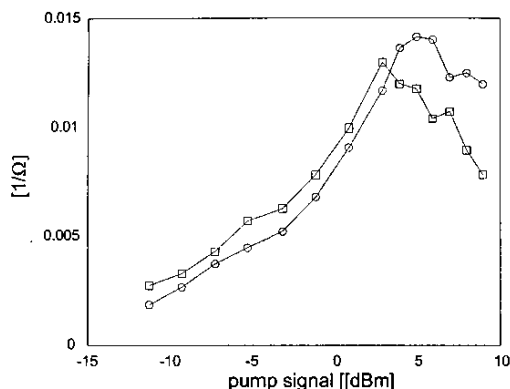


Fig. 6. Magnitude of the coefficients:  $y_{2110}$  (squares),  $y_{2101}$  (circles) at  $V_d = 3$  V,  $V_g = -0.45$  V.

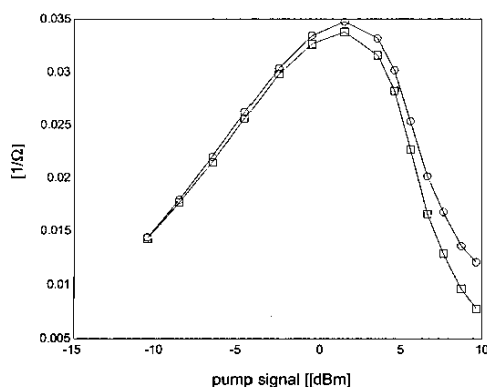


Fig. 7. Magnitude of the coefficients:  $y_{2110}$  (squares),  $y_{2101}$  (circles) at  $V_d = 3$  V,  $V_g = -0.85$  V.

Fig. 7 reports analogous behavior for the bias point  $V_g = -0.85$  V. From the graphs, we note a slight difference in the  $y_{2110}$  and  $y_{2101}$  coefficients. This behavior is related to the nonlinear capacitances. Moreover, there are no significant differences between maximum values obtained at different bias conditions. However, note that a lower pump signal is required to reach this condition. With that in mind, the bias point  $V_g = -0.85$  V is seen as a suitable bias point for up- and down-conversion. Fig. 8 shows the MCG in the up- and down-conversion, as evaluated by (2), for the bias point  $V_g = -0.85$  V. The shape and the optimum power level are the same as in Fig. 7, which confirms the importance of this parameter as a figure of merit for the device operating as a frequency converter. The maximum values of the MCG, calculated by the (2), is in the range of 15 dB in down-conversion and 35 dB in up-conversion for the case of a 0 dBm pump signal level. Hence, the up- and down-conversions are characterized in this way, so that the differences between the two conversion mechanisms are mainly due to different values of the input and output impedances as defined by (2).

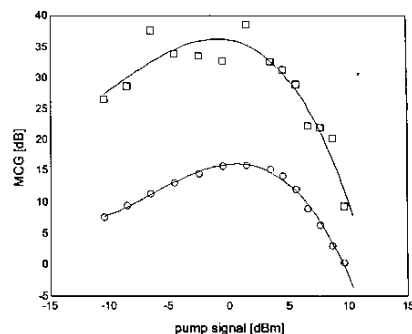


Fig. 8. Magnitude of the maximum conversion gain between 5.4 GHz and 600 MHz as a function of the pump signal, at  $V_d = 3$  V,  $V_g = -0.85$  V, in down-conversion (circle) and up-conversion (square) (solid curves represent a polynomial fitting).

#### IV. CONCLUSION

We have introduced a technique to experimentally derive the conversion matrix from vectorial large-signal measurements. The method has been applied to investigate the conversion properties of a 2.5  $\mu\text{m}$  PHEMT as functions of the pump signal and bias point. The experimental results allow us to determine the pump level, the bias voltage and the terminations for optimal design. We believe that the method constitutes an effective improvement in the behavioral description of active devices for mixer design.

#### REFERENCES

- [1] D. Barataud, et al. "Measurement and Control of Current/Voltage Waveforms of Microwave Transistors Using a Harmonic Load-Pull System for the Optimum Design of High Efficiency Power Amplifiers," *IEEE Trans. on Instrumentation and Measurement*, Vol. 48, No. 4, pp. 835-842, August 1999.
- [2] J. Verspecht, P. Van Esch, "Accurately characterizing of hard nonlinear behaviour of microwave components by the Nonlinear Network Measurement System: introducing the nonlinear scattering function", *Proc. INNMC'98*, pp. 17-26, Duisburg, October 1998.
- [3] J. A. Jargon, K. C. Gupta, D. Schreurs, and D. C. DeGroot, "Developing Frequency-Domain Models for Nonlinear Circuits Based on Large-Signal Measurements," *Proceedings of the XXVIIIth General Assembly of the International Union of Radio Science*, CD-ROM A1.O.6, Maastricht, the NETHERLANDS, Aug. 2002.
- [4] D. Schreurs et al, "Direct Extraction of the Non-Linear Model for Two-Port Devices from Vectorial Non-Linear Network Analyzer Measurements," *European Microwave Conf.*, pp. 921-926, 1997.
- [5] S. A. Maas, *Microwave Mixers*, Norwood MA: Artech House, 1986.
- [6] E. Vandamme, J. Verspecht, F. Verbeyst, M. Vanden Bossche, "Large-Signal Network Analysis – A Measurement Concept to Characterize Nonlinear Devices and Systems" <http://wireless.agilent.com/l sna/l snainain.htm>.